Quantum state preparation of a mechanical resonator using an optomechanical geometric phase

2013 New J. Phys. 15 043025

(http://iopscience.iop.org/1367-2630/15/4/043025)

New Journal of Physics
The open access journal for physics

Quantum state preparation of a mechanical resonator using an optomechanical geometric phase

K E Khosla[1,3], M R Vanner[1,2], W P Bowen[1] and G J Milburn[1]

[1] Center for Engineered Quantum Systems, University of Queensland, St Lucia 4072, Australia

[2] Vienna Center for Quantum Science and Technology (VCQ) and Faculty of Physics, University of Vienna, Boltzmanngasse 5, A-1090 Vienna, Austria

E-mail: k.khosla@uq.edu.au

New Journal of Physics **15** (2013) 043025 (11pp)
Received 27 September 2012
Published 17 April 2013
Online at http://www.njp.org/
doi:10.1088/1367-2630/15/4/043025

Abstract. We theoretically show that a geometric phase, generated by a sequence of four optomechanical interactions can be used to generate or increase nonlinearities in the evolution of a mechanical resonator. Interactions of this form lead to new mechanisms for preparing mechanical squeezed states of motion, and the preparation of non-classical states with significant Wigner negativity.

Contents

[3] Author to whom any correspondence should be addressed.

1. Introduction

The geometric phase is a phase imparted on the wavefunction of a quantum state by driving a system about a circuit [1]. Within quantum optics this phase has been widely used to create logic gates for quantum computing [2–4], but has received little attention in optomechanics. Some notable exceptions come from recent proposals that have considered the effect of a geometric phase involving mechanical oscillators coupled to a qubit [5] or light [6], however not for mechanical state engineering. In this paper we consider an optomechanical system [7–12] with a time dependent optical drive [9, 12, 13] that, via the optomechanical interactions, traverses a closed loop in phase space thus imparting a geometric phase onto the mechanical element.

In an optomechanical system, the radiation pressure force due to light in an optical resonator can be used to accelerate a mechanical resonator. Driving the optical resonator with a suitable sequence of laser pulses can be used to manipulate the motion of the mechanics. In our scheme, strong mechanical nonlinearity is generated with a sequence of four pulsed optomechanical interactions in a measurement free process. During this sequence the optical field makes a circuit in phase space and the mechanical oscillator obtains a phase proportional to the area enclosed within the loop [1], i.e. a Berry phase. It is shown how this phase produces an effective nonlinear potential for the mechanical resonator from the otherwise linear optomechanical radiation pressure interaction. We then discuss how this mechanical nonlinearity can be used for quantum state preparation of the mechanical oscillator. Our full protocol takes place within a small fraction of one period of the mechanical oscillator, and is hence robust against rethermalization and decoherence (similar to [12]).

2. Model

We model the optomechanical system as an optical cavity coupled linearly to the position of a mechanical element. The interaction Hamiltonian for such a system is given by $H_{\rm I} = \hbar g_0 a^\dagger a\sqrt{2}X_{\rm M}$, where g_0 is the interaction rate, $\hbar$ is the reduced Planck's constant, a, $(a^\dagger)$ and b, $(b^\dagger)$ are the annihilation (creation) operators of the optical and mechanical field respectively. The $\sqrt{2}$ arises from our definition of $X_{\rm M} = (b + b^\dagger)/\sqrt{2}$.

The Langevin equation of motion for a is given by $\dot{a}(t) = -{\rm i}g_0 a(t)X_{\rm M} - \kappa a(t) + \sqrt{2\kappa}a_{\rm in}(t)$ where $a_{\rm in}$ is the field entering the cavity and κ is the cavity decay rate. For the following the intracavity field is taken to be on resonance and κ is taken to be large compared to the mechanical frequency. The optical field is written as a noise operator $\bar{a}$ about a coherent amplitude $\alpha(t) = \langle a(t)\rangle$, such that $a(t) = \alpha(t) + \bar{a}(t)$. The coherent amplitude follows the classical equation of motion for a field in a cavity with input $\alpha_{\rm in}(t)$, $\dot{\alpha} = -\kappa\alpha(t) + \sqrt{2\kappa}\alpha_{\rm in}(t)$.[4] The mechanical period $T_{\rm M}$ is assumed much larger than the pulse envelope $\alpha(t)$, so the dynamics of the mechanical oscillator may be neglected, i.e. $X_{\rm M}(t) = X_{\rm M}$. The noise operator follows the equation of motion

$$\dot{\bar{a}}(t) = -{\rm i}g_0[\alpha(t) + \bar{a}(t)]X_{\rm M} - \kappa\bar{a}(t) + \sqrt{2\kappa}\bar{a}_{\rm in}(t). \tag{1}$$

For the rest of this work, the optomechanical system is taken to be in the weak coupling regime, $g_0 \ll \kappa$. In this limit coupling between the mechanical element and optical vacuum field

[4] If the pulse were detuned from the cavity resonance, the coherent amplitude inside the cavity would be smaller, reducing the optomechanical interaction.

(the $\bar{a}(t)X_{\mathrm{M}}$ term) is negligibly weak and is dropped. The Hamiltonian that gives the simplified equation of motion is given by

$$H_{\mathrm{I}}/\hbar = g_0|\alpha(t)|^2 X_{\mathrm{M}} + g_0|\alpha(t)|(\mathrm{e}^{\mathrm{i}\theta}\bar{a}^{\dagger} + \mathrm{e}^{-\mathrm{i}\theta}\bar{a})\sqrt{2}X_{\mathrm{M}}, \tag{2}$$

where θ is the phase angle of the coherent amplitude. For a single pulse θ may be taken to be arbitrary but it is kept here as it will become important when considering multiple pulses. The first term generates a classical momentum imparted to the oscillator, $P_{\mathrm{M}} \rightarrow P_{\mathrm{M}} - g_0 \int \mathrm{d}t|\alpha(t)|^2$, where the integral is over the duration of the pulse and therefore proportional to the input pulse intensity. The unitary operator for the quantum interaction in equation (2) is given by

$$U(X_{\mathrm{L}}^{\theta}) = \exp\left[-\mathrm{i}\chi X_{\mathrm{M}} X_{\mathrm{L}}^{\theta} - \mathrm{i}g_0 \int \mathrm{d}t|\alpha(t)|^2 X_{\mathrm{M}}\right], \tag{3}$$

where $\chi = \sqrt{2}g_0 \int \mathrm{d}t|\alpha(t)|$ and $X_{\mathrm{L}}^{\theta} = (\bar{a}\,\mathrm{e}^{-\mathrm{i}\theta} + \bar{a}^{\dagger}\,\mathrm{e}^{\mathrm{i}\theta})/\sqrt{2}$ is an arbitrary optical quadrature. In calculating this unitary operator we have used the assumption that the mechanical period T_{M} is large compared to the temporal width (σ) of the pulse.

We now consider a sequence of four pulsed optomechanical interactions. The same pulse is recycled and undergoes four separate interactions. After each interaction the pulse is displaced in optical phase space such that each interaction has a different phase angle X_{L}^{θ}. Let the four optical quadratures used be $\{X_{\mathrm{L}}, P_{\mathrm{L}}, -X_{\mathrm{L}}, -P_{\mathrm{L}}\}$, with $X_{\mathrm{L}} = (\bar{a} + \bar{a}^{\dagger})/\sqrt{2}$, $P_{\mathrm{L}} = (\bar{a} - \bar{a}^{\dagger})/(\sqrt{2}\mathrm{i})$. For each interaction the pulse has been taken to have the same temporal profile. This is valid as long as the pulse width is much larger than the cavity decay rate $\sigma \gg \kappa^{-1}$. Under this assumption the cavity filed follows the input pulse, $\alpha(t) = \alpha_{\mathrm{in}}(t)\sqrt{2/\kappa}$. The Baker–Campbell–Hausdorff formula [14] is used to calculate the effective unitary operator for the four interactions

$$\begin{aligned} U_{\mathrm{eff}} &= U(-P_{\mathrm{L}})U(-X_{\mathrm{L}})U(P_{\mathrm{L}})U(X_{\mathrm{L}}) \\ &= \exp[-\mathrm{i}\chi^2 X_{\mathrm{M}}^2]\exp\left[-4\mathrm{i}g_0 \int \mathrm{d}t|\alpha(t)|^2 X_{\mathrm{M}}\right]. \end{aligned} \tag{4}$$

The first exponential in U_{eff} is a geometric phase dependent on the position quadrature of the mechanical oscillator. The second exponential is the dynamical phase [15] which would be present in the corresponding classical system. The dynamical phase is simply a sum of the momentum displacements the mechanical oscillator receives from each pulsed interaction. The geometric phase can be seen as a momentum displacement proportional to the mechanical position, $U_{\mathrm{eff}}^{\dagger} P_{\mathrm{M}} U_{\mathrm{eff}} = P_{\mathrm{M}} - \chi^2 X_{\mathrm{M}} - 4g_0 \int |\alpha(t)|^2 \mathrm{d}t$. The momentum of the oscillator is displaced and becomes correlated with the position, resulting in a squeezed quadrature in the final mechanical state.

One may show more generally that the area of an arbitrary closed circuit will appear in this exponential. The proof (also discussed in [5]) goes as follows: consider an arbitrary closed curve in phase space made by a sequence of optomechanical interactions. One may break this sequence into a series of small but finite phase space displacements and then write the overall unitary operator as a product of each displacement. Converting the product of displacements to a single operator will generate a phase depending on each successive displacement. Taking the continuum limit where the number of displacements becomes infinite, one may convert the phase term into an integral and then use Stokes theorem to show the integral to be the area enclosed by the path.

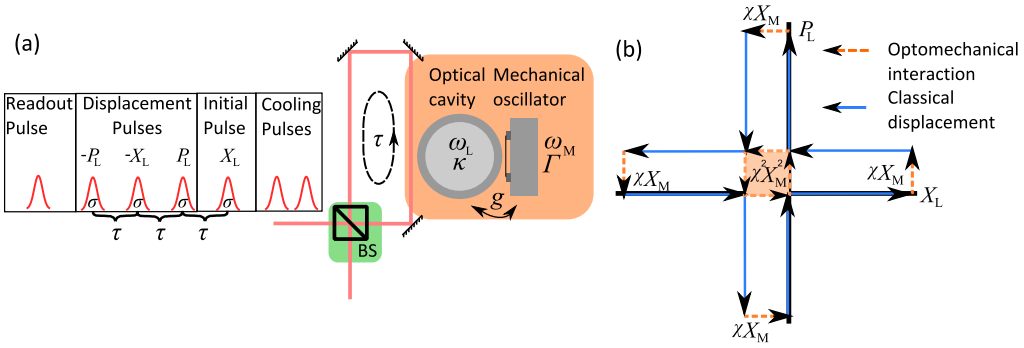

Figure 1. (a) A schematic for an experimental protocol to realize mechanical nonlinearity via an optomechanical geometric phase. The required pulse sequence is shown entering the beamsplitter. The first two pulses cool the mechanical oscillator close to the ground state. The initial pulse enters the large fiber cavity via the highly reflective beamsplitter. The following three displacement pulses only displace the coherent amplitude of the pulse inside the large fiber cavity, leaving the noise operator unchanged, effectively meaning the noise operator of the first pulse interacts with the mechanics four times. (b) The evolution of the optical field in phase space. The solid lines show the coherent drive, with the dashed lines (each of length χX_{M}) representing the optomechanical interaction. The geometric phase arises due to a sequence of four optomechanical interactions, hence it is the area enclosed by these mechanical position dependent optical phase shifts (dashed lines) that generate the geometric phase. The coherent optical amplitude drives the optomechanical system and gives rise to the dynamical phase, i.e. the momentum transfer to the mechanical resonator from each optical pulse.

3. Experimental scheme

Figure 1(a) shows a schematic of one possible experiment to realize the geometric phase. Two pulses separated by one quarter of a mechanical period are used to cool the mechanical element (as outlined in [12]), leaving it in a thermal state with a mean phonon occupation lower than that of the bath. Following the cooling pulses, a coherent laser pulse of temporal width σ enters a large fiber cavity with round trip time τ via a highly reflective beamsplitter. The pulse interacts with the mechanical oscillator via evanescent coupling from a toroidal cavity [16] with decay rate κ before exiting the toroidal cavity back into the large fiber cavity. As the pulse passes the highly reflective beamsplitter, its coherent amplitude is displaced in optical phase space leaving the noise operator fixed. The optical displacement is performed at the highly reflective beamsplitter using a second, phase controlled laser pulse to displace away the coherent amplitude, and displace up in an orthogonal quadrature. The pulse then repeats the optomechanical interactions and displacement three more times to give the four pulses sequence. Figure 1(b) shows the field inside the toroidal cavity over the experimental protocol.

The first pulse correlates the phase quadrature of the light, P_{L}, with the position of the mechanics, X_{M}. The first optical displacement changes the coherent amplitude of the pulse from the X_{M} to the P_{L} quadrature, before the second optomechanical interaction. For the second interaction, X_{L} is correlated with the mechanical position as it used to be P_{L} before the

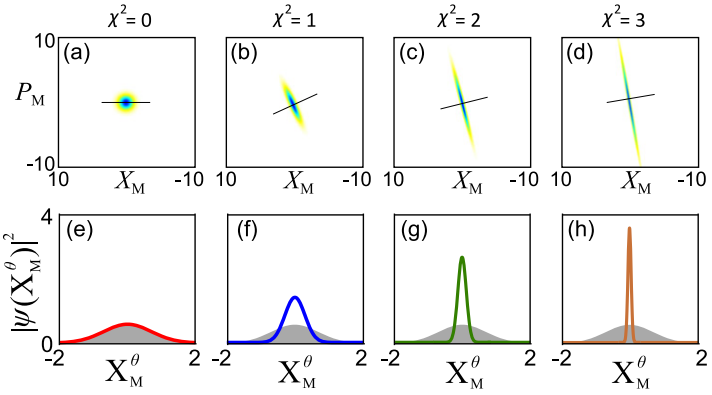

Figure 2. (a)–(d) Effect of a sequence of four optomechanical interactions on the Wigner function of the mechanical oscillator, initially prepared in the ground state. The squeezed quadrature (X_{M}^{θ}) is marked by a line in each graph. This quadrature is maximally squeezed at an angle $\tan\theta = \sqrt{\chi^4+1} - \chi^2$ to the X_{M} quadrature. (e)–(h) The probability amplitude for the squeezed quadrature compared to the ground state value (shown in gray).

displacement. During the second interaction the back action of X_{L} on the mechanical resonator effectively correlates the momentum of the oscillator with its position. As the position does not change over these interactions, correlating the momentum with the position produces a mechanical squeezed state. At this point the optical field is still correlated with the mechanical state, however, after the following two pulsed interactions, the correlation is undone such that the final optical pulse is uncorrelated with the mechanical state, leaving the final state disentangled. A readout pulse can now be sent into the cavity to measure the mechanical element and verify the mechanical state.

To generate the geometric phase we require $\kappa^{-1} < 4\sigma < \tau \ll T_{\mathrm{M}}$. Setting $\kappa^{-1} < 4\sigma$ ensures the field inside the toroid follows input field. Constraining $4\sigma < \tau$ ensures that each successive pulse decays out of the cavity prior to the next pulse entering. Consequently interference between successive pulses can be neglected. Finally requiring $\tau \ll T_{\mathrm{M}}$ means the mechanics remains near motionless during the four pulse protocol. The mechanical Q must be high enough such that on average much less than 1 phonon is exchanged with the bath over the time scale of the protocol.

Figure 2 shows the effect of the four pulse sequence on a mechanical oscillator initially prepared in the ground state, demonstrating how correlating X_{M} and P_{M} leads to a squeezed mechanical state of motion. Increasing the coupling strength χ benefits the protocol in two ways. Firstly it increases the effect of squeezing in the oscillator. Secondly it rotates the state so the squeezed quadrature aligns closer with the position quadrature, so that less time is required before the state can be verified (see section 4), and therefore the degradation in the squeezing due to thermalization will be reduced.

4. Experimental parameters

The previous section showed that under ideal conditions the geometric phase can be used to produce squeezed mechanical states. In this section we will consider experimental technicalities

such as thermalization of the mechanical oscillator, optical losses and possible non-closing of the optical phase space loop. Each of these effects will have a detrimental effect on the squeezing of the mechanical oscillator.

Optical losses effect this protocol in two ways. Firstly, classical attenuation from the beamsplitter will result in the phase space loop remaining unclosed after the four pulse sequence. This can be corrected by changing either the amplitude or phase of each subsequent displacement to counteract the attenuation. Secondly, optical losses will also add amplitude-noise back action on the momentum of the mechanics. In the absence of vacuum noise entering each cycle, any back action on the momentum in the X_{L} (P_{L}) pulse will be reversed by the $-X_{\mathrm{M}}$ ($-P_{\mathrm{M}}$) pulse. However when vacuum noise is introduced at the beamsplitters, the amplitude noise in the $-X_{\mathrm{M}}$ pulse will no longer perfectly cancel the amplitude noise from the X_{M} pulse. Unlike the attenuation of the classical amplitude this mechanism cannot be easily corrected for in the protocol.

For a beamsplitter with 99:1 reflectivity for the optical displacement, we expect $1-0.99^2 \approx 2\%$ vacuum noise to be imparted onto the oscillator from each of the $X_{\mathrm{L}}, -X_{\mathrm{L}}$ and $P_{\mathrm{L}}, -P_{\mathrm{L}}$ pulse pairs. Quantifying the total loss over a single cycle (beamsplitter, fiber loss, input–output coupling etc—modeled as an effective beamsplitter with vacuum input) by η, then $1-\eta^2$ vacuum noise would be introduced to the oscillator. The square arises from the fact the pulse must circulate twice before it cancels the noise, e.g. the noise imparted from the X_{M} pulse will only be canceled two cycles later from the $-X_{\mathrm{M}}$ pulse. Even after correcting for the effect of losses, classical fluctuations in the pulse intensities could result in non-closure of the phase space loop. If the loop is not closed after the four pulse sequence, the effective geometric phase[5] unitary operator is given by $U = \exp[-\mathrm{i}X_{\mathrm{M}} \sum_j \chi_j X_{\mathrm{L}}^{\phi_j} - \mathrm{i}\chi^2 X_{\mathrm{M}}^2]$, where here $\chi^2 = \sum_{j=1,\, j<k\leq 4}^{j=4} \chi_j \chi_k [X_{\mathrm{M}}^{\phi_k}, X_{\mathrm{M}}^{\phi_j}]/(2\mathrm{i})$ and $\chi_i = 4g_0\sqrt{N_i \sigma_i \sqrt{\pi/2}/\kappa}$ for a Gaussian pulse with temporal width σ_i and N_i photons. The second term in the above operator is the geometric phase. The first term leaves the mechanical element in an entangled state with the light after the interaction. This can be viewed as a momentum displacement on the mechanics that depends on the optical field, $D(-\mathrm{i}\chi^{\mathrm{fin}} X_{\mathrm{L}}^{\phi^{\mathrm{fin}}})$, where χ^{fin} is the displacement in the $X_{\mathrm{L}}^{\phi^{\mathrm{fin}}}$ quadrature that defines the final optical state. If χ^{fin} and ϕ^{fin} are unknown, the final state must be averaged over possible values, reducing the squeezing. A homodyne measurement of the light lost from the beamsplitter will give an estimate of χ^{fin} and ϕ^{fin}, meaning this error can be accounted for retrospectively. Note laser phase noise will change the direction of each displacement pulse which may result in non-closure of the optical phase space loop. Figure 3 shows how $\chi^{\mathrm{fin}} \neq 0$ changes the squeezed state. Note for when χ^{fin} is small, the squeezing is only slightly affected.

Even if classical drifts in the optical displacements are corrected for, vacuum noise introduced by losses in the feedback loop can cause non-closure resulting in a mixed mechanical state. For a single pass efficiency in the fiber loop η, the cancellation of noise between pairs of displacement measurements (e.g. X_{M} and $-X_{\mathrm{M}}$) will be degraded by a factor $1-\eta^2$, leading to a loop non-closure of $2-2\eta$. For realistic inefficiencies in the range of 10% (corresponding to $2-2\times 1.8 = 0.2$—i.e. 20% vacuum noise) the loop non-closure due to non-cancellation of noise is negligible, i.e. $\chi^{\mathrm{fin}} = 4g_0\sqrt{0.2\sigma\sqrt{\pi/2}/\kappa} \ll 1$. Hence the squeezing is not significantly affected by the addition of vacuum noise.

The following considers the effect of thermalization on the mechanical squeezed state. Thermalization can have two detrimental effects. Firstly, phonon exchange with the bath during

[5] I.e. ignoring the dynamical phase.

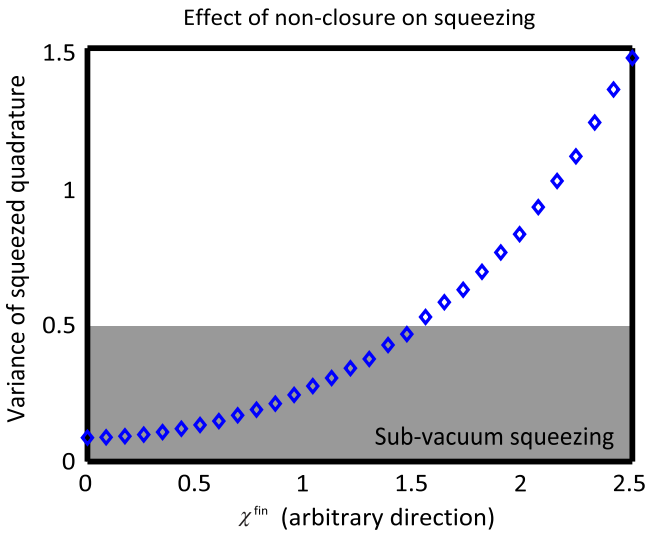

Figure 3. Effect of non-closure of the loop on the squeezed state for a fixed $\chi^2 = 1$. χ^{loss} is the magnitude of non-closure in an unknown quadrature $X_{\text{L}}^{\phi_{\text{loss}}}$. Once the variance of the squeezed state goes above one, squeezing becomes impossible as the amount of noise added from the non-closure of the loop is larger than the ground state variance.

the four pulse sequence will render the dynamics over the pulse sequence non-unitary and change the final mechanical state. Secondly phonons that enter during the time scale required for the squeezed quadrature to rotate into the measurable position quadrature will degrade the squeezing. The first of these effects can be neglected since the four pulses can be very closely spaced with only a short delay between them. For example, for a mechanical oscillator with resonance frequency $\omega_{\text{M}} = 24\,\text{kHz}$, and quality factor $Q = 10^5$, the pulse duration should be $\sigma \simeq 10^{-8}\,\text{s}$, such that the time for four pulses (on the order of $10^{-7}\,\text{s}$), is much smaller than the time scale for one phonon to enter the oscillator, $1/(\Gamma\bar{N}) \approx 10^{-5}\,\text{s}$ at 1 K. Consequently, only thermal phonon exchange after the state has been prepared will be considered. The mechanical oscillator was modeled as an oscillator with noised added only on the momentum quadrature. For small times $t \ll \omega_{\text{m}}^{-1}$ one may neglect the oscillator decay. The equation of motion was then solved to find the variance $\langle \Delta^2 X_{\text{M}} \rangle = \langle X_{\text{M}}^2 \rangle - \langle X_{\text{M}} \rangle^2$ of the position as a function of time

$$\begin{aligned}\langle \Delta^2 X_{\text{M}} \rangle = {} & [\langle X_{\text{M}}^2(0) \rangle \cos^2(\omega t) + \langle {P_{\text{M}}}^2(0) \rangle \sin^2(\omega t)] \\ & + \langle X_{\text{M}}(0) P_{\text{M}}(0) + P_{\text{M}}(0) X_{\text{M}}(0) \rangle \sin(\omega t) \cos(\omega t) \\ & + \Gamma \left(\bar{N} + \frac{1}{2} \right) \left[\frac{t}{2} - \frac{\sin(2\omega t)}{4\omega} \right], \end{aligned} \tag{5}$$

where $\langle X_{\text{M}}^2(0) \rangle = \bar{N} + \frac{1}{2}$, $\langle P_{\text{M}}^2(0) \rangle = (\bar{N} + \frac{1}{2})(1 + 4\chi^4)$ and $\langle X_{\text{M}}(t) P_{\text{M}}(0) + P_{\text{M}}(0) X_{\text{M}}(0) \rangle = -4\chi^2 (\bar{N} + \frac{1}{2})$ are the expectation values after the geometric phase has been applied.

To minimize the initial phonon number before the four pulse sequence we envisage cooling via pulsed measurement as outlined in [12]. In this protocol, two pulses separated by 1/4 of the mechanical period are used to measure the oscillator in two orthogonal quadratures, leading to

a low entropy state. The result in [12] shows an effective thermal phonon number of

$$\bar{N}_{\rm eff} \simeq \frac{1}{2}\left(\sqrt{1+\frac{1}{\chi^4}+\frac{\pi\bar{N}}{Q\chi^2}}-1\right), \tag{6}$$

where $\chi = 4g_0\sqrt{N_{\rm p}\sigma\sqrt{\frac{\pi}{2}/\kappa}}$ (the same χ used elsewhere). This gives $\bar{N}_{\rm eff} \simeq 10$ for a 1 mm, 24 kHz SiN resonator with $Q \approx 10^5$ and photon number $N_{\rm p} = |\alpha|^2 \approx 10^6$. Using the SiN string mechanical oscillators considered in this paper, the effective phonon number is achievable for resonance frequencies of $\omega_{\rm M} < 70$ kHz and length $L < 5$ mm with a maximum incident photon flux of $\dot{N}_{\rm p} = 10^{16}$ Hz (≈2 mW at 630 nm). Although this is the initial phonon occupation, the bath occupation remains at $\bar{N} \approx 10^5$.

SiN strings present a particularly attractive mechanical oscillator, high mechanical quality factors of up to 7×10^6 have been observed, and the mechanical resonance frequency may be tuned via tensioning [17, 18]. The protocol requires the mechanical period to be large compared to all other characteristic time scales. From this constraint we will limit the following analysis to low frequency, $\omega_{\rm m} = 1$–70 kHz, SiN strings. From [18], the expected Q factor of a stressed SiN string of dimensions $L \times h \times w$ is

$$Q = \left[\frac{(n\pi)^2 E h^2}{12SL^2} + 1.0887\sqrt{\frac{E}{S}}\frac{h}{L}\right]^{-1} Q_{\rm Bending} \tag{7}$$

with $E = 241 \pm 4$ GPa the Young's modulus of SiN, $Q_{\rm Bending} = 17\,000$ the quality factor related to bending damping mechanisms and $S = 4\omega_{\rm m}^2 L^2 \rho_{\rm SiN}$ the tensile stress of SiN (with density $\rho_{\rm SiN}$) in the high stress limit.

The optomechanical coupling rate g_0 is calculated from evanescently coupled SiN string coupling rate $G = 200\,{\rm MHz\,nm^{-1}}$ [19] and the oscillators zero point motion: $g_0 = Gx_0 = G\sqrt{\hbar/(2m\omega_{\rm M})}$ with m the effective mass of the mode. The pulse width and optical cavity decay rate are defined by $T_{\rm m} = 10^{-3}\sigma = 5/\kappa$ to satisfy the experimental requirements.

After preparing the mechanical quantum state with the four pulse sequence, it may be characterized with a measurement pulse. Figures 4(a) and (b) show the temporal progression of the variance over various time scales after the four pulse sequence. Figure 4(c) shows a plot of $\langle\Delta^2 X_{\rm M}\rangle$ as a function of length and resonance frequency of a SiN string at 1 K with cross section 157 nm × 3 μm. These two parameters may be chosen independently by tensioning the string to the desired frequency. The dashed line of $Q = 7 \times 10^6$ is just larger than the highest observed Q in a SiN string [18]. This figure shows it is experimentally feasible to achieve quantum squeezing for a wide range of geometries with the best squeezing of $\Delta^2 X_{\rm M} \approx 10^{-2}$ predicted for a 3.5 mm long oscillator with 20 kHz resonance frequency and $Q = 5 \times 10^6$. For all points in this figure, the initial state had an effective phonon number of $N_{\rm eff} = 10$ phonons; the maximum intracavity photon number to achieve such cooling was 10^6 photons which is readily achieved.

The $X_{\rm M}^2$ appearing in the unitary operator is a result of the geometric phase changing a linear optomechanical interaction into an effective quadratic potential. If the mechanics was instead quadratically coupled to the light field [10, 16, 20, 21] ($H_{\rm I} = g_0\hbar a^\dagger a X_{\rm M}^2$), the result would be a factor $X_{\rm M}^4$ in the unitary operator—increasing the nonlinearity present in the Hamiltonian to fourth order. In this case we may view the interaction as a position-cubed dependent displacement, $U = \exp[-{\rm i}\chi^2 X_{\rm M}^4] = D(-{\rm i}\chi^2 x^3)$ correlating the momentum of the oscillator with the cube of its position. With large enough quadratic coupling, this

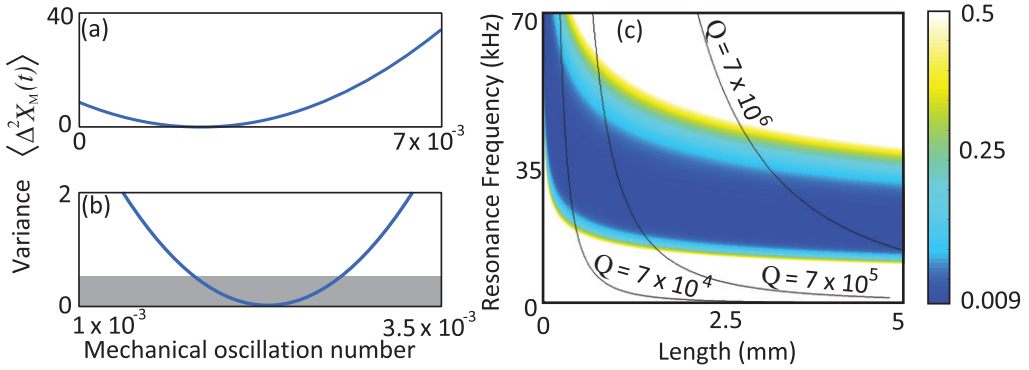

Figure 4. Progression of the variance of the mechanical oscillator over two time scales: (a) free evolution immediately after the four pulse sequence, (b) explicitly showing the squeezed region and (c) experimentally observable squeezing generated via a geometric phase of an oscillator initially cooled to $N_{\text{eff}} = 10$. The color scale gives the variance in the position quadrature over one decay time of the oscillator. A value less than 0.5 indicates squeezing below the ground state variance. The plot color axis is truncated at 0.5.

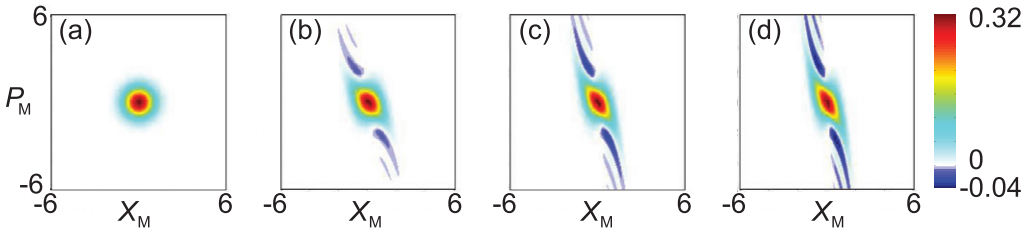

Figure 5. Wigner functions of the mechanical state after a geometric phase interaction on the mechanical ground state of motion with a quadratically coupled mechanical oscillator for values of (a) $\chi^2 = 0$, (b) $\chi^2 = 0.066$, (c) $\chi^2 = 0.133$, (d) $\chi^2 = 0.2$. The momentum becomes correlated with the cube of the position—this can be seen in the Wigner function follows a profile proportional to $-x^3$ with negativity arising in the concave sections of the curve.

provides an avenue to generate quantum states of the oscillator involving significant Wigner negativity, see figure 5. Wigner negativity is an unambiguous and sufficient indicator of non-classicality [22, 23]. Exploring such states experimentally is of vital importance to determine the feasibility of mechanical oscillators as elements in quantum applications and to gain a deeper empirical understanding of the quantum-to-classical transition.

5. Conclusion

In summary, we have proposed an experiment that uses a geometric phase to generate nonlinearity and non-classical motional states of a mechanical resonator. This provides a new tool in optomechanics for quantum state engineering of mechanical oscillators. We have shown our method to be both experimentally feasible and robust to optical and mechanical noise sources.

Acknowledgments

This research was funded by the Australian Research Council Center of Excellence CE110001013.

References

[1] Berry M V 1987 The adiabatic phase and Pancharatnam's phase for polarized light *J. Mod. Opt.* **34** 1401–7
[2] Sørensen A and Mølmer K 2000 Entanglement and quantum computation with ions in thermal motion *Phys. Rev.* A **62** 022311
[3] Milburn G J, Schneider S and James D F V 2000 Ion trap quantum computing with warm atoms *Fortschr. Phys.* **48** 801–10
[4] Leibfried D *et al* 2003 Experimental demonstration of a robust, high-fidelity geometric two ion-qubit phase gate *Nature* **422** 412–5
[5] Vacanti G, Fazio R, Kim M S, Palma G M, Paternostro M and Vedral V 2012 Geometric phase kickback in a mesoscopic qubit-oscillator system *Phys. Rev.* A **85** 022129
[6] Pikovski I, Vanner M R, Aspelmeyer M, Kim M S and Brukner Č 2012 Probing Planck-scale physics with quantum optics *Nature Phys.* **8** 393–7
[7] Bose S, Jacobs K and Knight P L 1999 Scheme to probe the decoherence of a macroscopic object *Phys. Rev.* A **59** 3204–10
[8] Mancini S, Giovannetti V, Vitali D and Tombesi P 2002 Entangling macroscopic oscillators exploiting radiation pressure *Phys. Rev. Lett.* **88** 120401
[9] Marshall W, Simon C, Penrose R and Bouwmeester D 2003 Towards quantum superpositions of a mirror *Phys. Rev. Lett.* **91** 130401
[10] Thompson J D, Zwickl B M, Jayich A M, Marquardt F, Girvin S M and Harris J G E 2008 Strong dispersive coupling of a high-finesse cavity to a micromechanical membrane *Nature* **452** 72–5
[11] Eichenfield M, Chan J, Camacho R M, Vahala K J and Painter O 2009 Optomechanical crystals *Nature* **462** 78–82
[12] Vanner M R, Pikovski I, Cole G D, Kim M S, Brukner Č, Hammerer K, Milburn G J and Aspelmeyer M 2011 Pulsed quantum optomechanics *Proc. Natl Acad. Sci. USA* **108** 16182–7
[13] Jacobs K 2007 Engineering quantum states of a nanoresonator via a simple auxiliary system *Phys. Rev. Lett.* **99** 117203
[14] Dynkin E B 1947 Calculation of the coefficients in the Campbell–Hausdorff formula *Dokl. Akad. Nauk. SSSR (N.S.)* **57** 323–6
[15] Berry M V 1984 Quantal phase factors accompanying adiabatic changes *Proc. R. Soc. Lond.* **392** 45–57
[16] Anetsberger G, Arcizet O, Unterreithmeier Q P, Rivière R, Schliesser A, Weig E M, Kotthaus J P and Kippenberg T J 2009 Near-field cavity optomechanics with nanomechanical oscillators *Nature Phys.* **5** 909–14
[17] Verbridge S S, Shapiro D F, Craighead H G and Parpia J M 2007 Macroscopic tuning of nanomechanics: substrate bending for reversible control of frequency and quality factor of nanostring resonators *Nano Lett.* **7** 1728–35
[18] Schmid S, Jensen K D, Nielsen K H and Boisen A 2011 Damping mechanisms in high-Q micro and nanomechanical string resonators *Phys. Rev.* B **84** 165307
[19] Anetsberger G, Weig E M, Kotthaus J P and Kippenberg T J 2011 Cavity optomechanics and cooling nanomechanical oscillators using microresonator enhanced evanescent near-field coupling *C. R. Phys.* **12** 800–16
[20] Jayich A M, Sankey J C, Zwickl B M, Yang C, Thompson J D, Girvin S M, Clerk A A, Marquardt F and Harris J G E 2008 Dispersive optomechanics: a membrane inside a cavity *New J. Phys.* **10** 095008

[21] Purdy T P, Brooks D W C, Botter T, Brahms N, Ma Z-Y and Stamper-Kurn D M D M 2010 Tunable cavity optomechanics with ultracold atoms *Phys. Rev. Lett.* **105** 133602

[22] Bužek V and Knight P L 1995 Quantum interference, superposition states of light and nonclassical effects *Prog. Opt.* **34** 1–158

[23] Kenfack A and Zyczkowski K 2004 Negativity of the Wigner function as an indicator of non-classicality *J. Opt. B: Quantum Semiclass. Opt.* **6** 396–404